Nonequilibrium condensation process of a holographic superconductor in de Rham-Gabadadze-Tolley massive gravity

Ran Li[*] and Yujia Zhao[†]

Institute of Theoretical Physics, College of Physics, Henan Normal University, Xinxiang 453007, China

(Received 16 April 2019; published 23 August 2019)

We study the nonequilibrium condensation process of a holographic s-wave superconductor constructed in the background of de Rham-Gabadadze-Tolley massive gravity theory. When the temperature is lower than a critical value, this model has an asymptotic anti–de Sitter (AdS) bald black hole solution and a black hole solution with nontrivial scalar hair, which can be identified as the normal phase and the superconducting phase in boundary theory, respectively. We consider Gaussian-type perturbation of a scalar field on the background of bald AdS black hole spacetime, and we numerically solve the full nonlinear dynamics of the gravitational system in the bulk. With the full time-dependent solution of the gravitational system, we observe a dynamical process from the perturbed bald AdS black hole to the black hole with scalar hair. According to holographic duality, this process can be regarded as the dynamical phase transition process from normal state to s-wave superconducting state in boundary theory. We also investigate the time evolution of the superconducting condensate operator and clarify how the condensation process from the far-from-equilibrium state proceeds in boundary theory. By fitting the evolution data of the superconducting order parameter at early time, we show that the initial nonequilibrium condensation process can be predicted by linear quasinormal modes of scalar field perturbation on the background of the bald AdS black hole. Finally, we study the time evolution of the event and apparent horizons.

DOI: 10.1103/PhysRevD.100.046018

I. INTRODUCTION

The application of anti–de Sitter/conformal field theory (AdS/CFT) correspondence [1–3] to study strongly coupled quantum field theory has received increasing attention over the past two decades. Within the framework of holographic duality, the strongly coupled quantum many body systems in condensed matter physics can be simply described by the classical gravity theory on the AdS spacetime. A recent review studying the properties of quantum matter by using the holographic method can be found in Ref. [4]. Specifically, in the seminal work of Hartnoll *et al.* [5,6], the holographic model of Einstein-Maxwell-charged complex scalar field theory was constructed to capture the essential properties of a superconductor with an s-wave order parameter. It is shown that, due to the instability of the Reissner-Nordström-AdS (RN-AdS) black hole below the critical temperature, the scalar field will condense into a nontrivial configuration in the bulk, and a nonvanishing vacuum expectation value of the charged s-wave condensate operator will emerge in boundary theory. The RN-AdS black hole and hairy black hole in gravitational theory are dual to the normal and superconducting phases of a superconductor in the boundary. One can also refer to Ref. [7] for a overview of some holographic superconductor models with s-wave, p-wave, and d-wave orders.

However, the construction of superconducting system in this way omitted the key ingredient of condensed matter systems: the lattice. The absence of an underlying lattice means that the boundary system is homogeneous, with perfect translational symmetry, and the charged particles cannot dissipate their momentum. As a consequence, there is a delta function in the ac conductivity at zero frequency. This implies that the dc conductivity is infinite even in the normal phase of the superconductor. One way to avoid this unwanted result is to treat the charge carriers as probes, i.e., as a small part in a larger system of neutral fields represented by the bulk geometry where their momentum can be absorbed [8–11]. Another way is to introduce spatial inhomogeneities that break translational invariance explicitly. In Refs. [12,13], when considering the periodic gravitational background to simulate the lattice in condensed matter systems, it is shown that the zero frequency delta function resulting from translational symmetry is broadened and that the dc conductivity is finite.

Vegh put forward a simple proposal of taking de Rham-Gabadadze-Tolley (dRGT) massive gravity theory [14] as an alternative holographic framework for describing translational symmetry breaking and momentum dissipation [15]. A massive gravity theory can be constructed by

[*]liran@htu.edu.cn
[†]1399365255@qq.com

modifying general relativity with consistent interaction terms that are interpreted as mass terms for the gravitons. Fierz and Pauli [16] constructed a linear massive gravity theory by adding interaction terms in the linearized level of general relativity. Unfortunately, the massive gravity theory of Fierz and Pauli suffered from the van Dam–Veltman–Zakharov discontinuity problem on the linear level [17,18], and the Boulware-Deser ghost problem on the nonlinear level [19,20]. Recently, de Rham, Gabadadze, and Tolley constructed a nonlinear massive gravity theory, dubbed dRGT massive gravity theory [14], where the Boulware-Deser ghost was eliminated by introducing higher order interaction terms into the Einstein-Hilbert action.

Within this framework, bulk gravitons are assumed to have a mass term, which can serve as a coarse-grained description of the momentum dissipation effect of a lattice. The charged asymptotic AdS black hole solution in dRGT massive gravity theory was constructed in Ref. [15], and the conductivity was shown to have a Drude peak that approaches a delta function in the massless gravity limit. Recently, a holographic superconductor model in the background of dRGT massive gravity theory was constructed by Zeng and Wu in Ref. [21]. It was shown that, when the temperature is lower than a critical value, the model has an asymptotic AdS bald black hole solution and a black hole solution with nontrivial scalar hair, which can be identified as the normal phase and the superconducting phase in boundary theory, respectively. The ac conductivity of the superconducting state exhibits a Drude peak at low frequency followed by a power-law fall.

In modern condensed matter physics experiments, it is now possible to drive a system to a far-from-equilibrium state by a quantum quench [22]. So, one might raise the natural and legitimate question of studying the far-from-equilibrium dynamics of the superconductor model from the viewpoint of holographic duality. In the past few years, this topic has attracted a lot of attention [23]—for example, the quantum quench of a superconducting AdS soliton [24], holographic thermalization [25–27], the formation of topological defects [28,29], a periodically driven holographic superconductor [30], nonlinear transport in holographic superconductors [31], the critical exponents of nonequilibrium phase transitions [32], and the nonequilibrium condensation process of s-wave superconductors [33–36] and p-wave superconductors [37].

It should be noted that the studying of the nonequilibrium condensation process of holographic superconductors was initiated by Murata *et al.* in Ref. [33], and it was then generalized to other models. However, as far as we know, all of the previous work investigated the nonequilibrium condensation process of holographic superconductors without momentum dissipation. In this work, we will focus on the nonequilibrium condensation process of a holographic s-wave superconductor constructed in dRGT massive gravity theory [21], which is a holographic superconductor model with momentum dissipation as introduced previously. By perturbing the bald AdS black hole spacetime with the Gaussian-type wave package and numerically solving the full nonlinear dynamics of the bulk gravitational system, we observe a nontrivial process from the perturbed bald AdS black hole to the black hole with scalar hair. In terms of holographic duality, this process is regarded as the dynamical phase transition process from normal state to s-wave superconducting state in boundary theory. By means of investigating the time evolution of the superconducting condensate operator, we will clarify how the condensation process from the far-from-equilibrium state proceeds in boundary theory. It is shown that the initial nonequilibrium condensation process can be predicted by the linear quasinormal modes of scalar field perturbation on the background of the bald AdS black hole. We will also address the question of the time evolution of the event and apparent horizons. Our numerical simulations indicate that the nonequilibrium condensation process of holographic superconductor with momentum dissipation is qualitatively consistent with that of superconductor without momentum dissipation.

This paper is organized as follows. In Sec. II, we present the setup of the holographic s-wave superconductor model in dRGT massive gravity. The details for describing the nonequilibrium condensation process are also given in that section. In Sec. III, we exhibit the numerical results of the nonequilibrium condensation process, including the dynamics of the bulk scalar field, the dynamics of order parameter, quasinormal modes of scalar perturbation, and the evolution of the areas of apparent and event horizons. Finally, we conclude this paper with some discussions in Sec. IV.

II. HOLOGRAPHIC SETUP AND NUMERICAL DETAILS

In this section, we start by introducing the holographic setup of superconductor models in nonlinear massive gravity theory, which we will be studied in this paper. After writing down the action and equations of motion of the bulk theory, we proceed by discussing the bald black hole solution that describes the normal phase of the boundary system, and by deriving the asymptotic expansions for the bulk fields at the AdS boundary. At last, we will briefly describe the field redefinition, the boundary conditions, the initial conditions, and the numerical details used to obtain time-dependent solutions of bulk equations.

A. Action

The total action of the holographic superconductor model of concern in this paper is given by

$$I = I_G + I_M, \tag{1}$$

where we have denoted the action of nonlinear ghost-free massive gravity as I_G, and the action of $U(1)$ gauge field coupled with charged complex scalar field as I_M.

For our purposes, we consider the recently proposed $(3+1)$-dimensional dRGT ghost-free massive gravity with the action [14]

$$I_G = \frac{1}{2\kappa^2}\int d^4x\sqrt{-g}\left[R + \frac{6}{L^2} + m_g^2\sum_{i=1}^{4} c_i\mathcal{U}_i(g,f)\right], \quad (2)$$

where c_i are constants and m_g is the mass of the graviton. In this case, besides the usual dynamical metric g, the theory depends on a fixed rank-2 symmetric tensor f, which is called the reference metric. The well-known Boulware-Deser ghost was eliminated by introducing higher order interaction terms $\mathcal{U}_i(g,f)$. These terms are defined as the symmetric polynomials of the eigenvalues of the 4×4 matrix $\mathcal{K}^\mu_\nu = \sqrt{g^{\mu\lambda}f_{\lambda\nu}}$,

$$\begin{aligned}
\mathcal{U}_1 &= [\mathcal{K}],\\
\mathcal{U}_2 &= [\mathcal{K}]^2 - [\mathcal{K}^2],\\
\mathcal{U}_3 &= [\mathcal{K}]^3 - 3[\mathcal{K}][\mathcal{K}^2] + 2[\mathcal{K}^3],\\
\mathcal{U}_4 &= [\mathcal{K}]^4 - 6[\mathcal{K}^2][\mathcal{K}]^2 + 8[\mathcal{K}^3][\mathcal{K}] + 3[\mathcal{K}^2]^2 - 6[\mathcal{K}^4],
\end{aligned}$$

where $\mathcal{K}^2{}_{\mu\nu} = \mathcal{K}_{\mu\alpha}\mathcal{K}^\alpha{}_\nu$, and where the rectangular brackets denote traces—for example, $[K] = K^\mu_\mu$. As $m_g \to 0$, the action recovers to the usual Einstein-Hilbert action with cosmological constant.

The holographic superconductor model in nonlinear ghost-free massive gravity [21] can be constructed by introducing a $U(1)$ gauge field coupled with a charged complex scalar field with the action

$$I_M = -\frac{1}{2\kappa^2}\int d^4x\sqrt{-g}\left[\frac{1}{4}F_{\mu\nu}F^{\mu\nu} + |\nabla\Psi - iqA\Psi|^2 + m^2|\Psi|^2\right], \quad (3)$$

where the $U(1)$ gauge field strength is defined by $F_{\mu\nu} = \nabla_\mu A_\nu - \nabla_\nu A_\mu$, and where m and q are the mass and $U(1)$ charge of the complex scalar field Ψ, respectively. Hereafter, without loss of generality, we take the unit of $L = 1$.

B. Equations of motion

From the total action (1), by varying with respect to metric, complex scalar field, and gauge potential, one can get an Einstein equation, a charged Klein-Gordon equation, and a Maxwell equation as follows,

$$R_{\mu\nu} - \frac{1}{2}g_{\mu\nu}R - 3g_{\mu\nu} + m_g^2 X_{\mu\nu} = T^{\mathrm{EM}}_{\mu\nu} + T^{\Psi}_{\mu\nu}, \quad (4)$$

$$(\nabla_\mu - iqA_\mu)(\nabla^\mu - iqA^\mu)\Psi - m^2\Psi = 0, \quad (5)$$

$$\nabla_\mu F^{\mu\nu} = iq[\Psi^*(\nabla^\nu - iqA^\nu)\Psi - \Psi(\nabla^\nu + iqA^\nu)\Psi^*], \quad (6)$$

where the stress-energy tensors of the matter sector are given by

$$T^{\mathrm{EM}}_{\mu\nu} = \frac{1}{2}\left(g^{\sigma\rho}F_{\mu\sigma}F_{\nu\rho} - \frac{1}{4}g_{\mu\nu}F^{\rho\sigma}F_{\rho\sigma}\right), \quad (7)$$

$$\begin{aligned}
T^{\Psi}_{\mu\nu} &= \frac{1}{2}[(\nabla_\mu\Psi - iqA_\mu\Psi)(\nabla_\nu\Psi^* + iqA_\nu\Psi^*) + \text{c.c.}]\\
&\quad - \frac{1}{2}g_{\mu\nu}|\nabla\Psi - iqA\Psi|^2 - \frac{1}{2}g_{\mu\nu}m^2|\Psi|^2.
\end{aligned} \quad (8)$$

Following Refs. [15,21], we are interested in the case of a spatial reference metric in the basis (t,z,x,y)

$$f_{\mu\nu} = \mathrm{diag}(0,0,1,1). \quad (9)$$

In this case, $X_{\mu\nu}$ is given by

$$\begin{aligned}
X_{\mu\nu} &= \frac{c_1}{2}(\mathcal{K}_{\mu\nu} - [\mathcal{K}]g_{\mu\nu})\\
&\quad - c_2\left(\mathcal{K}^2{}_{\mu\nu} - [\mathcal{K}]\mathcal{K}_{\mu\nu} + \frac{1}{2}g_{\mu\nu}([\mathcal{K}]^2 - [\mathcal{K}^2])\right).
\end{aligned} \quad (10)$$

In order to utilize the characteristic solution scheme to study the nonlinear dynamics of this model, following the general approach of Ref. [38], we take the metric *Ansatz* as

$$ds^2 = -\frac{1}{z^2}[F(v,z)dv^2 + 2dvdz] + \Phi(v,z)^2(dx^2 + dy^2), \quad (11)$$

where $F(v,z)$ and $\Phi(v,z)$ are nontrivial functions depending on the time v and the holographic bulk direction z. We work in a axial gauge where the *Ansatz* of gauge field and scalar field can be written as

$$A = \alpha(v,z)dt, \qquad \Psi = \psi(v,z). \quad (12)$$

With these choices, one can derive the equations of motion as follows:

$$\Phi'' + \frac{2}{z}\Phi' + \frac{1}{2}\Phi|\psi'|^2 = 0, \quad (13)$$

$$\alpha'' + 2\left(\frac{1}{z} + \frac{\Phi'}{\Phi}\right)\alpha' + \frac{iq}{z^2}(\psi\psi'^* - \psi^*\psi') = 0, \quad (14)$$

$$\begin{aligned}
&(D\Phi)' + \frac{\Phi'}{\Phi}D\Phi - \frac{\Phi}{8z^2}(z^4\alpha'^2 + 2m^2|\psi|^2 - 12)\\
&\quad + \frac{m_g^2}{2z^2}\left(c_1 + \frac{c_2}{\Phi}\right) = 0,
\end{aligned} \quad (15)$$

$$(D\psi)' + \frac{\Phi'}{\Phi} D\psi + \frac{D\Phi}{\Phi}\psi' + \frac{1}{2z^2}(iqz^2\alpha' + m^2)\psi = 0, \tag{16}$$

$$\left(z^2\left(\frac{F}{z^2}\right)'\right)' - \left(\frac{4}{\Phi}\right)' D\Phi + \frac{m_g^2}{z^2\Phi}\left(c_1 + \frac{2c_2}{\Phi}\right) - z^2\alpha'^2 - (\psi'^* D\psi + \psi' D\psi^*) = 0, \tag{17}$$

and

$$2z^2(D\alpha)' + (4z^2\Phi^{-1}D\Phi + z^2F' - 2zF)\alpha' + 2iq(\psi^* D\psi - \psi D\psi^*) = 0, \tag{18}$$

$$zD^2\Phi - FD\Phi + \frac{1}{2}z(\Phi D\psi D\psi^* + D\Phi F') + \frac{F^2}{8}(4\Phi' + z\Phi|\psi'|^2 + 2z\Phi'') = 0, \tag{19}$$

where the prime denotes the derivative with respect to the radial coordinate z, and where derivative operator D is defined as

$$D\Phi = \partial_v\Phi - \frac{1}{2}F\partial_z\Phi, \qquad D^2\Phi = \partial_v(D\Phi) - \frac{1}{2}F\partial_z(D\Phi),$$
$$D\alpha = \partial_v\alpha - \frac{1}{2}F\partial_z\alpha, \qquad D\psi = \partial_v\psi - \frac{1}{2}F\partial_z\psi - iq\alpha\psi,$$
$$D\psi^* = \partial_v\psi^* - \frac{1}{2}F\partial_z\psi^* + iq\alpha\psi^*. \tag{20}$$

Here the operator $(\partial_v - \frac{1}{2}F\partial_z)$ is the derivative along the radial outgoing null geodesics. In the limit $m_g \to 0$, the equations of motion go back to those obtained in Ref. [33]. In the numerical calculation, we regard Eqs. (13)–(17) as evolution equations and Eqs. (18) and (19) as constraint equations in the following.

C. Normal phase solution

According to AdS/CFT correspondence, it is well known that the normal phase of boundary field theory is described by a bulk static AdS black hole solution with vanishing scalar field. This static AdS black hole solution [15] can be obtained by solving the equations of motion directly, which is given by

$$F = 1 + \frac{1}{2}c_1 m_g^2 z + c_2 m_g^2 z^2 - 2Mz^3 + \frac{1}{4}Q^2 z^4,$$
$$\Phi = \frac{1}{z}, \qquad \alpha = Qz, \qquad \psi = 0. \tag{21}$$

In the limit $m_g \to 0$, the solution reduces to the Reissner-Nordström-AdS black hole solution with planar horizon. Parameters M and Q are related to the mass and charge of the black hole, respectively. The event horizon is located at $z = z_+$, determined by $F(z_+) = 0$. In terms of the horizon radius z_+, we can rewrite M as

$$M = \frac{1}{2z_+^3}\left(1 + \frac{1}{2}c_1 m_g^2 z_+ + c_2 m_g^2 z_+^2 + \frac{1}{4}Q^2 z_+^4\right). \tag{22}$$

The Hawking temperature of the black hole is given by

$$T = -\frac{1}{4\pi}\frac{dF}{dz}\bigg|_{z=z_+} = \frac{12 + 4c_1 m_g^2 z_+ + 4c_2 m_g^2 z_+^2 - Q^2 z_+^4}{16\pi z_+}. \tag{23}$$

The vanishing configuration of the complex scalar field indicates that the order parameter of boundary dual theory is also null. The hairless black hole solutions which are characterized by the two parameters M and Q are identified as the dual bulk description of normal phase in boundary theory. As discussed in the next section, this solution is unstable when the temperature is below a critical temperature T_c. This implies that there exists a hairy black hole solution with nontrivial scalar configuration when the temperature is smaller that the critical temperature. The hairy black hole solution which can be regarded as the superconducting phase was already obtained in Ref. [21]. The instability is identified as the phase transition from metal to superconducting in dual boundary theory.

In the following, we will study the dynamics process of this superconducting phase transition from the viewpoint of gravity aspect. By considering the slightly perturbed hairless black hole spacetime as initial data, and by studying the full time-dependent solutions of the equations of motion, we will find that the system settles to the final state of the hairy black hole at late time when the initial black hole temperature is smaller than the critical temperature T_c.

D. Asymptotic expansion

Now let us exhibit the asymptotic form for the bulk fields at the AdS boundary in order to clarify the boundary conditions for the time evolution. Hereafter, we set the mass of the complex vector field as $m^2 = -2$. Then the asymptotical behavior for the scalar field near the AdS boundary takes the form of

$$\psi(v, z) = \psi_1(v)z + \psi_2(v)z^2 + \cdots. \tag{24}$$

According to the holographic dictionary, if we take ψ_1 as the source, ψ_2 is then identified as the vacuum expectation value of the operator $\hat{O}_2$ in boundary dual field theory, up to a normalization constant. Since we want the condensate to turn on without being sourced, we set $\psi_1 = 0$.

It should be noted that the diffeomorphism and $U(1)$ gauge symmetries are not completely fixed by the *Ansätze* (11) and (12). There are residual gauge symmetries given by

$$\frac{1}{z}\to\frac{1}{z}+g(v),\qquad \alpha\to\alpha+\partial_v\theta(v),\qquad \psi\to\psi e^{iq\theta(v)}. \tag{25}$$

In asymptotic expansion, the residual gauge freedoms are represented by $\Phi_0(v)$ and $\alpha_0(v)$, which are the zero order terms of the bulk functions $\Phi(v)$ and $\alpha(v)$. The freedom of $\Phi_0(v)$ can be used to fix the position of the apparent horizon at a constant radial coordinate during the evolution, as in Ref. [38]. However, we do not explore the time evolution of $\Phi_0(v)$ and fix the gauge freedoms by setting $\Phi_0(v)=\alpha_0(v)=0$.

By fixing the gauge as described above and solving the equations of motion order by order, one can find that the expansion coefficients $F_i(v)$, $\Phi_i(v)$, $\alpha_i(v)$, and $\psi_i(v)$ can all be determined by $\psi_2(v)$, except for $F_3(v)$ and $\alpha_1(v)$. The results are as follows,

$$F(v,z)=1+\frac{1}{2}c_1m_g^2z+c_2m_g^2z^2-2Mz^3+\cdots, \tag{26}$$

$$\Phi(v,z)=\frac{1}{z}-\frac{1}{6}|\psi_2|^2z^3+\cdots, \tag{27}$$

$$\alpha(v,z)=Qz+\frac{iq}{12}(\psi_2^*\dot\psi_2-\psi_2\dot\psi_2^*)z^4+\cdots, \tag{28}$$

$$\psi(v,z)=\psi_2(v)z^2+\dot\psi_2(v)z^3+\cdots, \tag{29}$$

where the raised dot means $\frac{d}{dv}$.

It should be noted that the asymptotic expansion gives just the time derivative of $F_3(v)$ and $\alpha_1(v)$ as $\dot F_3(v)=\dot\alpha_1(v)=0$, which implies that $F_3(v)$ and $\alpha_1(v)$ are invariant during the dynamical evolution process. In fact, $F_3(v)$ and $\alpha_1(v)$ are related to the mass and charge of the system. We have used the notations $F_3(v)=-2M$ and $\alpha_1(v)=Q$ in the above expansion. Hence the constants M and Q represent the Arnowitt-Deser-Misner mass and the charge of the initial black hole, respectively. At last, the function $\psi_2(v)$ is the only unknown function which shall be determined by the numerical solution.

E. Field redefinition and boundary conditions

With the asymptotic expansion exhibited in the last subsection, one can see clearly that the variable $S(v,z)$ is divergent at the AdS boundary $z=0$. This leads to the divergence of the variable $DS(v,z)$. However, the divergent form of these variables is fully determined by the asymptotic expansion at the AdS boundary. In order to remove the divergence of fields at the AdS boundary, we make the fields redefinition as follows:

$$\begin{aligned}
F&=1+\frac{1}{2}c_1m_g^2z+c_2m_g^2z^2+z\hat F,\\
\Phi&=\frac{1}{z}+z^2\hat\Phi,\\
\alpha&=\hat\alpha,\\
\psi&=z^2\hat\psi,\\
D\Phi&=\frac{1}{2z^2}+\frac{1}{4}c_1m_g^2z+\frac{1}{2}c_2m_g^2z^2+z\widehat{D\Phi},\\
D\psi&=z\widehat{D\psi}.
\end{aligned} \tag{30}$$

By definition, the hatted fields then have regular asymptotic behavior. The resulting $z\to0$ boundary conditions can be obtained from the asymptotic expansion (26)–(29) directly:

$$\begin{aligned}
\hat\Phi(v,0)&=0,\qquad \hat\Phi'(v,0)=-\frac{1}{6}|\psi_2|^2,\\
\hat\alpha(v,0)&=0,\qquad \hat\alpha'(v,0)=Q,\\
\widehat{D\Phi}(v,0)&=-M,\\
\widehat{D\psi}(v,0)&=-\psi_2,\\
\hat F(v,0)&=\hat F'(v,0)=0.
\end{aligned} \tag{31}$$

The corresponding evolution equations for the hatted fields are obtained by substituting the redefinitions into the equations of motion. We do not write the resulting lengthy expressions here.

F. Initial conditions

To extrapolate the time-dependent solution of the system, one is also required to specify the initial condition. The static bald black hole solution of the equations of motion is the Reissner-Nordström-AdS black hole solution with planar horizon described above. We take this bald black hole as the initial spacetime background. Firstly, we should specify M and Q of the initial black hole. By using the following scaling symmetry,

$$\begin{aligned}
&(v,z,x,y)\to(kv,kz,kx,ky),\\
&F\to F,\qquad \Phi\to\Phi/k,\\
&\alpha\to\alpha/k,\qquad \psi\to\psi,\\
&M\to M/k^3,\qquad Q\to Q/k^3,\qquad T\to T/k,
\end{aligned} \tag{32}$$

we can set the initial black hole horizon radius to unity without loss of generality. Then the mass and temperature of the black hole are given by

$$\begin{aligned}
M&=\frac{1}{2}\left(1+\frac{1}{2}c_1m_g^2+c_2m_g^2+\frac{1}{4}Q^2\right),\\
T&=\frac{12+4c_1m_g^2+4c_2m_g^2-Q^2}{16\pi},
\end{aligned} \tag{33}$$

which implies that the initial spacetime background is completely determined by the parameter Q, or equivalently the temperature of initial bald black hole.

As for the initial data of scalar field $\hat{\psi}$, we consider the Gaussian-type perturbation on the Reissner-Nordström-AdS spacetime as

$$\hat{\psi}(v=0,z)=\frac{\mathcal{A}}{\sqrt{2\pi}\delta}z^2\exp\left[-\frac{(z-z_m)^2}{2\delta^2}\right] \tag{34}$$

with $\mathcal{A}=0.01$, $\delta=0.05$, and $z_m=0.3$. However, our numerical simulations indicate that the final numerical results are independent of the choice of parameters A, δ, and z_m as long as the scalar perturbation is small enough and in the linear regime. We will exhibit our numerical results only for the initial data given by Eq. (34).

G. Numerical strategy

The procedure to solve the equations of motion (13)–(17) is described as follows. To begin with, we have to prepare the initial data of the complex scalar field $\psi(v=0,z)$ and the initial mass M and charge Q of the black hole background as described above. On the initial surface $v=0$, the field $\psi(v,z)$ represents the free initial data. Then all of the other fields can be solved from the equations of motion on the initial time slice.

In more detail, at the initial time, with the initial configuration ψ, we can get the functions Φ, α, $D\Phi$, $D\psi$, and F by solving the linear ordinary differential equations (13)–(17) subjected to the boundary conditions (31). In this process, we use the Chebyshev pseudospectral method to discretize the differential equations. The obtained linear algebraic equations can be straightforwardly solved by standard matrix methods. In this way, we can obtain all of the fields on the initial time surface. In terms of the definition of $D\psi$, we can also extract the time derivative $\partial_v\psi$ at this time step. Then we can calculate the configuration of scalar field ψ on the next time surface by using the fourth order Runge-Kutta method. By repeating the above procedure, we can obtain the full time-dependent numerical solution to the system. The constraint equations (18) and (19) are used to check the accuracy of the numerical solution.

III. NONEQUILIBRIUM CONDENSATION PROCESS

In this section, we will show the numerical results computed by the evolution strategy described in the previous section. As mentioned before, we have fixed the mass of the scalar field as $m^2=-2$. In this section, without loss of generality, we further fix the charge of the complex scalar filed as $q=1.5$. We will also choose the parameters as $c_1=-0.75$, $c_2=0$, and $m_g=1$ in the following. For this case, our numerical simulation indicates that the critical temperature of normal-superconductor phase transition in a dual system is given by $T_c=0.086825\sqrt{Q}$. When the initial temperature of black hole T is smaller than the critical temperature T_c, the complex scalar field perturbation grows exponentially and eventually approaches a nontrivial configuration in the bulk, which implies that the boundary system undergoes a phase transition from the normal phase to the s-wave superconducting phase. For the case of $T>T_c$, however, the initial scalar field perturbation decays to zero very quickly. This indicates that the initial bald black hole with temperature smaller than the critical temperature is stable under perturbation, and the normal-superconductor phase transition in the boundary system cannot happen.

A. Dynamics of the bulk field

In the left panel of Fig. 1, we show the dynamics of the amplitude of bulk fields $|\psi(v,z)|$ for $T/Tc=0.5$ at the initial state. The evolution of the complex scalar field

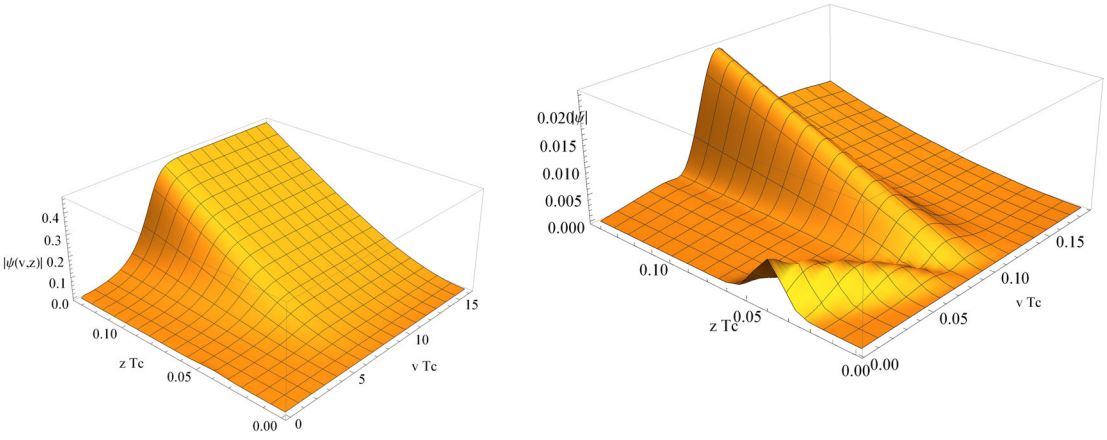

FIG. 1. The dynamics of the bulk scalar field for initial black hole temperature $T=0.5T_c$. (Left panel) Amplitude of the complex scalar field $|\psi(v,z)|$ as a function of vTc and zTc. It is shown that the amplitude grows exponentially till saturation. (Right panel) In order to focus on the behavior of the wave packet of the initial perturbation, we depict the amplitude $|\psi(v,z)|$ for $0\le vTc\le 0.15$.

shows three different stages, which is similar to the nonequilibrium condensation process in a holographic s-wave superconductor in Einstein gravity [33] and in a holographic p-wave superconductor in the Einstein-Proca gravity model [37]. As depicted in the right panel of Fig. 1, during the very early stage, $0 < vTc < 0.15$, much of the wave packet in the initial Gaussian-type perturbation is absorbed by the black hole horizon. During the second stage, $0.15 < vTc < 6$, the remnant of the wave packet, which is unstable, grows exponentially. This stage can be well predicted by the linear quasinormal mode analysis [33,36], as further discussed in the following subsections. For the third stage, the exponential growth is saturated by the nonlinear effect, and an equilibrium between the complex scalar field and the black hole is finally attained. It can be seen that the amplitude of bulk complex scalar field reaches a static hairy black hole solution with the nontrivial scalar configuration. This implies that the boundary system eventually evolves into an s-wave superconducting phase at late time.

B. Dynamics of the order parameter

In the following subsections, we will discuss some results that are relevant to the dual system in the boundary from the numerical time-dependent solutions in the AdS bulk. According to the AdS/CFT dictionary, in the present subsection, we first extract the nonlinear dynamics of the order parameter of the dual boundary field theory from the numerical solutions of the bulk fields.

The vacuum expectation value of the superconducting s-wave order parameter in dual theory is given by the asymptotic expansion coefficient $\psi_2(v)$ as follows,

$$\langle \mathcal{O}(v) \rangle = \sqrt{2}\psi_2(v), \tag{35}$$

when setting the source as $\psi_1(v) = 0$ in our numerical process.

In the left panel of Fig. 2, we depict the real part of asymptotic expansion coefficient $\psi_2(v)$ as a function of vTc with the initial black hole temperature $T/Tc = 0.5$. The imaginary part of $\psi_2(v)$ exhibits a similar behavior to the real part. The sharp signal appearing at small v is caused by the initial scalar perturbation. Then the time evolution of $\psi_2(v)$ shows two distinct stages. During the first stage, the amplitude of the oscillating ψ_2 grows exponentially due to the instability of the initial bald black hole, which is the expected behavior from the linear theory analysis. At the second stage, the exponential growth of $\psi_2(v)$ stops at late time, and the system reaches the final equilibrium state, during which the amplitude of the order parameter remains constant, as depicted in the right panel of Fig. 2.

The inset in the left panel of Fig. 2 shows the time evolution of the asymptotic expansion coefficient $\psi_2(v)$ at late time, which indicates the oscillating nature of the bulk scalar field when the final equilibrium state is reached. It can also be shown that the real part as well as the imaginary part of the asymptotic expansion coefficient $\psi_2(v)$ oscillates with a single frequency and with the opposite phases. This implies, when the real part of $\psi_2(v)$ is at a maximum of the magnitude of the amplitude, that the imaginary part has a vanishing amplitude. It should be emphasized that the vacuum expectation of the superconducting condensate operator is time independent in the final equilibrium state.

The true nature of the final equilibrium state can be further revealed by comparing the oscillating frequency of the bulk scalar field with the horizon electric potential of the final hairy black hole. By performing the Fourier transformation of the evolution data of the asymptotic expansion coefficient $\psi_2(v)$ at late time, we can estimate the oscillating frequency of the bulk scalar field when the final equilibrium state is reached, which is given by $\omega = 3.1283$. At late time, the geometry of the final hairy black hole is invariant with time. The event horizon radius z_{EH} of the final black hole is determined by the equation $F(v, z_{\mathrm{EH}}) = 0$. We can obtain the location of the event horizon by solving the equation after interpolating the

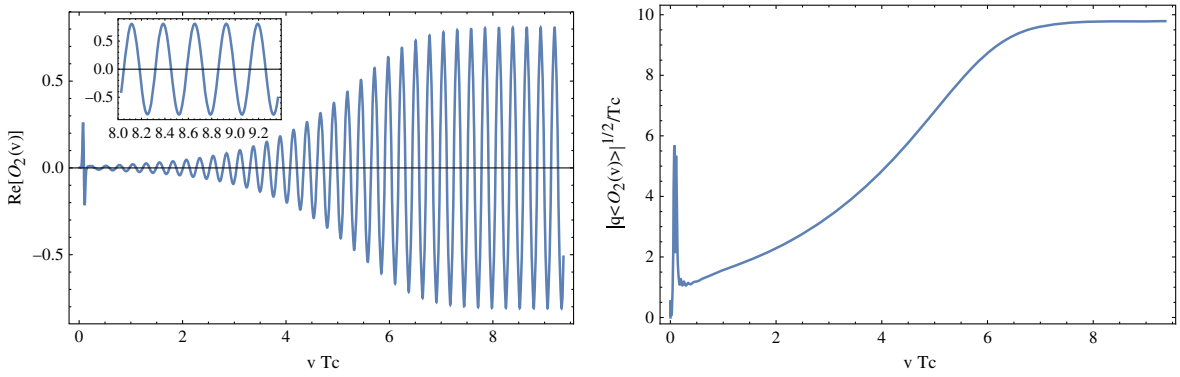

FIG. 2. (Left panel) Time evolution of the real part of asymptotic expansion coefficient $\psi_2(v)$ with $T/Tc = 0.5$. (Inset) The evolution at late time, which indicates the oscillating nature of complex scalar field when the final equilibrium state is reached. (Right panel) The time evolution of condensate operator $|\langle \mathcal{O}(v) \rangle|$.

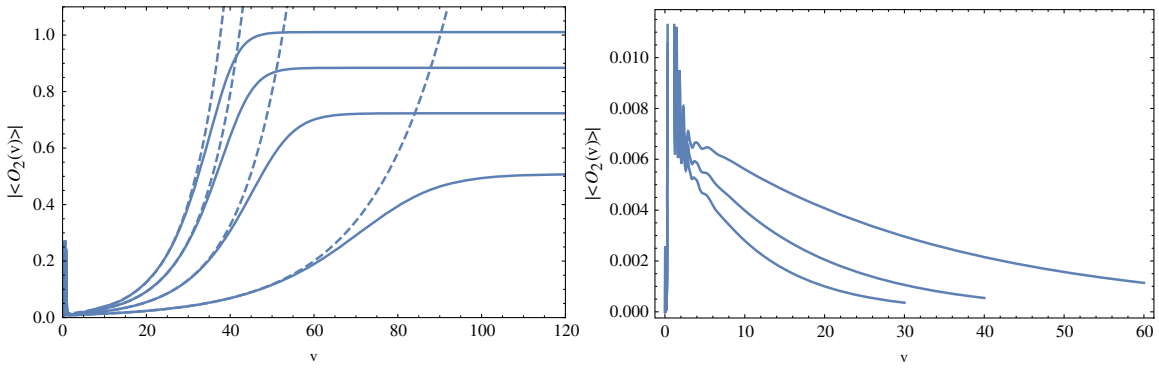

FIG. 3. The dynamics of the order parameter with different initial black hole temperatures. (Left panel) The solid curves from top to bottom correspond to $T/T_c = 0.2$, 0.4, 0.6, and 0.8, while the dashed curves represent the relaxation timescale by fitting the evolution data at early time. (Right panel) The different curves from top to bottom correspond to $T/T_c = 1.1$, 1.2, and 1.3.

metric function from the evolution data at late time. Then, by interpolating the electromagnetic potential from the evolution data, we can also determine the horizon electric potential α_H of the final hairy black hole. The oscillating frequency ω of the bulk scalar field at late time is nearly equal to the value of $q\alpha_H = 3.1248$, within acceptable numerical error. This result implies that the time-dependent configuration of the bulk system at late time can be transformed into the static black hole configuration with the vanishing electric potential at the horizon by a proper gauge transformation. This provides strong evidence that the equilibrium state obtained herein is the end point of the time evolution. This also implies that the final black hole with nontrivial scalar hair is stable.

C. Quasinormal modes of scalar field perturbation

In Fig. 3, we show the dynamics of the order parameter with different initial black hole temperatures. As mentioned before, our numerical results show the critical temperature is given by $T_c = 0.086825\sqrt{Q}$. This value is obtained by performing the numerical process repeatedly with different initial temperatures near this critical value. When $T < T_c$, the order parameter grows exponentially and eventually approaches a nontrivial value, as depicted in the left panel of Fig. 3. This result implies that the boundary system undergoes a phase transition from the normal phase described by a bald AdS black hole to the s-wave superconducting phase with a nontrivial complex scalar field configuration. From the left panel of Fig. 3, we can also conclude that the order parameter converges to its final value more slowly at higher initial temperatures, which indicates that the boundary system takes more time to approach the final equilibrium state at higher initial temperatures. For the case of $T > T_c$, on the other hand, the initial perturbations decay to zero very quickly, as shown in the right panel of Fig. 3.

TABLE I. The relaxation time and the fundamental quasinormal modes of scalar perturbation for the normal phase.

T/T_c	$-1/t_{\text{relax}}$	$\text{Im}(\omega)$
0.2	0.117839	0.118855
0.4	0.107671	0.109375
0.6	0.0895161	0.0901151
0.8	0.0533475	0.0536004
1.1	−0.0318835	−0.0318047
1.2	−0.102722	−0.102635
1.3	−0.0663066	−0.0662255

From these numerical results, one can conclude that the initial bald AdS black hole is unstable due to the so-called near-horizon instability when $T < T_c$ [39]. The initial growth rate at early time, when the perturbation remains small enough, should match the linearized quasinormal mode analysis. Now let us focus on the early time of the time evolution. Firstly, we can estimate the relaxation timescales at early time by fitting the time dependence of the order parameter as

$$|\langle \mathcal{O}(v)\rangle| \sim C\exp(-t/t_{\text{relax}}). \tag{36}$$

In Table I, we have listed the relaxation time for the initial bald AdS black hole at different temperatures.

It is well known that $-1/t_{\text{relax}}$ is just the imaginary part of the fundamental quasinormal mode. We have also computed the quasinormal modes of the scalar perturbation of the bald AdS black hole by using the *Mathematica* package made by Jansen [40]. The results are also listed in Table I for comparison. It can be observed that the results from fitting the time evolution data match with the linearized quasinormal mode quite well.

D. Evolution of event horizon and apparent horizon

In this subsection, we explore the time evolution of the apparent and event horizons. The apparent horizon of a black hole, which is defined as the location of the largest trapped surface, can be determined by the equation

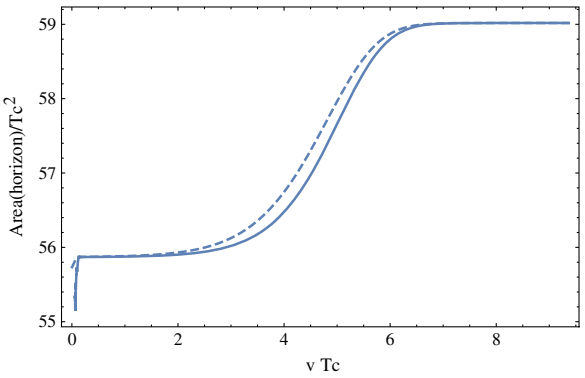

FIG. 4. The time evolution of the area of event and apparent horizons with the initial temperature $T/T_c = 0.5$. The solid and dashed curves correspond to the area of apparent and event horizons, respectively.

$$DS(v, z_{\mathrm{AH}}(v)) = 0. \tag{37}$$

One can also compute the event horizon $z_{\mathrm{EH}}(v)$ by solving the radial null geodesics equation

$$\dot{z}_{\mathrm{EH}}(v) = -\frac{1}{2}B(v, z_{\mathrm{EH}}(v)), \tag{38}$$

arising from $ds^2 = 0$, with the boundary condition at late time $B(v, z_{\mathrm{EH}}(v)) = 0$. Then the area of the apparent and event horizons can be calculated by the formula

$$\mathrm{Area\,(event/apparent\,horizon)} = S(v, z_{\mathrm{EH/AH}}(v))^2. \tag{39}$$

In Fig. 4, we show the time evolution of the area of the event and apparent horizons as a function of time vTc. It is clear that the monotonic increasing of the area of the horizons during the time evolution is consistent with the second law of black hole thermodynamics. Before the system settles to the final equilibrium state, the event horizon always has a larger area than that of the apparent horizon. At late time, the apparent horizon and the event horizon settle down to a constant value and coincide, which also implies the formation of a hairy black hole with nontrivial scalar hair.

IV. SUMMARY AND CONCLUSION

In summary, we study in this paper the nonequilibrium condensation process of a holographic superconductor with momentum dissipation, which is constructed in the framework of dRGT massive gravity theory. Using the characteristic evolution scheme for the AdS gravity, we obtain the time-dependent solution of full Einstein equations for the gravitational system in the bulk. The nonlinear dynamical process from the perturbed bald AdS black hole to the black hole with scalar hair is illustrated by using the numerical method. By AdS/CFT, the process is regarded as the dynamical phase transition process from normal state to s-wave superconducting state in the boundary. By studying the time evolution of the s-wave order parameter, we clarify how the condensation process from the far-from-equilibrium state proceeds. It is shown that the initial nonequilibrium condensation process can be predicted by the linear quasinormal modes of scalar field perturbation on the background of the bald AdS black hole. Finally, we also study the time evolution of the event and apparent horizons, which implies the formation of a hairy black hole with nontrivial scalar hair.

Our results show that the nonequilibrium condensation process of holographic superconductor with momentum dissipation is qualitatively consistent with that of a superconductor without momentum dissipation. The nonequilibrium condensation process of other holographic superconductors with momentum dissipation deserves further study in the future.

ACKNOWLEDGMENTS

This work is supported by the key research project of universities in Henan province under Grant No. 18A140005.

[1] J. M. Maldacena, The large-N limit of superconformal field theories and supergravity, Adv. Theor. Math. Phys. **2**, 231 (1998).
[2] S. S. Gubser, I. R. Klebanov, and A. M. Polyakov, Gauge theory correlators from non-critical string theory, Phys. Lett. B **428**, 105 (1998).
[3] E. Witten, Anti–de Sitter space and holography, Adv. Theor. Math. Phys. **2**, 253 (1998).
[4] S. A. Hartnoll, A. Lucas, and S. Sachdev, Holographic quantum matter, arXiv:1612.07324.
[5] S. A. Hartnoll, C. P. Herzog, and G. T. Horowitz, Building a Holographic Superconductor, Phys. Rev. Lett. **101**, 031601 (2008).
[6] S. A. Hartnoll, C. P. Herzog, and G. T. Horowitz, Holographic superconductors, J. High Energy Phys. 12 (2008) 015.
[7] R. G. Cai, L. Li, L. F. Li, and R. Q. Yang, Introduction to holographic superconductor models, Sci. China Phys., Mech. Astron. **58**, 060401 (2015).
[8] A. Karch and A. O'Bannon, Metallic AdS/CFT, J. High Energy Phys. 09 (2007) 024.

[9] T. Faulkner, N. Iqbal, H. Liu, J. McGreevy, and D. Vegh, From black holes to strange metals, arXiv:1003.1728.
[10] S. A. Hartnoll, J. Polchinski, E. Silverstein, and D. Tong, Towards strange metallic holography, J. High Energy Phys. 04 (2010) 120.
[11] S. A. Hartnoll and D. M. Hofman, Locally Critical Umklapp Scattering and Holography, Phys. Rev. Lett. **108**, 241601 (2012).
[12] G. T. Horowitz, J. E. Santos, and D. Tong, Optical conductivity with holographic lattices, J. High Energy Phys. 07 (2012) 168.
[13] G. T. Horowitz, J. E. Santos, and D. Tong, Further evidence for lattice-induced scaling, J. High Energy Phys. 11 (2012) 102.
[14] C. de Rham, G. Gabadadze, and A. J. Tolley, Resummation of Massive Gravity, Phys. Rev. Lett. **106**, 231101 (2011).
[15] D. Vegh, Holography without translational symmetry, arXiv:1301.0537.
[16] M. Fierz and W. Pauli, On relativistic wave equations for particles of arbitrary spin in an electromagnetic field, Proc. R. Soc. A **173**, 211 (1939).
[17] H. van Dam and M. J. G. Veltman, Massive and massless Yang-Mills and gravitational fields, Nucl. Phys. **B22**, 397 (1970).
[18] V. I. Zakharov, Linearized gravitation theory and the graviton mass, JETP Lett. **12**, 312 (1970).
[19] D. G. Boulware and S. Deser, Can gravitation have a finite range?, Phys. Rev. D **6**, 3368 (1972).
[20] D. G. Boulware and S. Deser, Inconsistency of finite range gravitation, Phys. Lett. **40B**, 227 (1972).
[21] H. B. Zeng and J.-P. Wu, Holographic superconductors from the massive gravity, Phys. Rev. D **90**, 046001 (2014).
[22] A. Polkovnikov, K. Sengupta, A. Silva, and M. Vengalattore, Colloquium: Nonequilibrium dynamics of closed interacting quantum systems, Rev. Mod. Phys. **83**, 863 (2011).
[23] H. Liu and J. Sonner, Holographic systems far from equilibrium: A review, arXiv:1810.02367.
[24] M. Bhaseen, J. P. Gauntlett, B. Simons, J. Sonner, and T. Wiseman, Holographic Superfluids and the Dynamics of Symmetry Breaking, Phys. Rev. Lett. **110**, 015301 (2013).
[25] X. Gao, A. M. Garcia-Garcia, H. B. Zeng, and H.-Q. Zhang, Normal modes and time evolution of a holographic superconductor after a quantum quench, J. High Energy Phys. 06 (2014) 019.
[26] A. M. Garca-Garca, H. B. Zeng, and H. Q. Zhang, A thermal quench induces spatial inhomogeneities in a holographic superconductor, J. High Energy Phys. 07 (2014) 096.
[27] A. Buchel, R. C. Myers, and A. van Niekerk, Nonlocal probes of thermalization in holographic quenches with spectral methods, J. High Energy Phys. 02 (2015) 017.
[28] J. Sonner, A. del Campo, and W. H. Zurek, Universal far-from-equilibrium dynamics of a holographic superconductor, Nat. Commun. **6**, 7406 (2015).
[29] P. M. Chesler, A. M. Garcia-Garcia, and H. Liu, Far-from-Equilibrium Coarsening, Defect Formation, and Holography, Phys. Rev. X **5**, 021015 (2015).
[30] W. J. Li, Y. Tian, and H.-B. Zhang, Periodically driven holographic superconductor, J. High Energy Phys. 07 (2013) 030.
[31] H. B. Zeng, Y. Tian, Z. Y. Fan, and C.-M. Chen, Nonlinear transport in a two dimensional holographic superconductor, Phys. Rev. D **93**, 121901 (2016); Nonlinear conductivity of a holographic superconductor under constant electric field, Phys. Rev. D **95**, 046014 (2017).
[32] H.-B. Zeng and H.-Q. Zhang, Universal critical exponents of nonequilibrium phase transitions from holography, Phys. Rev. D **98**, 106024 (2018).
[33] K. Murata, S. Kinoshita, and N. Tanahashi, Non-equilibrium condensation process in a holographic superconductor, J. High Energy Phys. 07 (2010) 050.
[34] X. Bai, B. H. Lee, M. Park, and K. Sunly, Dynamical condensation in a holographic superconductor model with anisotropy, J. High Energy Phys. 09 (2014) 054.
[35] Y. Liu, Y. Gong, and B. Wang, Non-equilibrium condensation process in holographic superconductor with nonlinear electrodynamics, J. High Energy Phys. 02 (2016) 116.
[36] R. Li, T. Zi, and H. Zhang, Nonlinear evolution dynamics of holographic superconductor model with scalar self-interaction, Phys. Rev. D **97**, 086001 (2018).
[37] R. Li, X. Chen, T. Zi, and H. Zhang, Nonequilibrium condensation process of a holographic p-wave superconductor, Phys. Rev. D **98**, 046024 (2018).
[38] P. M. Chesler and L. G. Yaffe, Numerical solution of gravitational dynamics in asymptotically anti–de Sitter spacetimes, J. High Energy Phys. 07 (2014) 086.
[39] O. J. C. Dias and R. Masachs, Hairy black holes and the end point of AdS_4 charged superradiance, J. High Energy Phys. 02 (2017) 128.
[40] A. Jansen, Overdamped modes in Schwarzschild–de Sitter and a Mathematica package for the numerical computation of quasinormal modes, Eur. Phys. J. Plus **132**, 546 (2017).